

COST – BENEFIT ANALYSIS OF THE AEROCAPTURE MISSION SET

Jeffery L. Hall*, Muriel A. Noca and Robert W. Bailey

Jet Propulsion Laboratory, California Institute of Technology, Pasadena, CA 91109

ABSTRACT

Calculations have been performed to quantify the cost and delivered mass advantages of aerocapture at all destinations in the Solar System with significant atmospheres. A total of eleven representative missions were defined for the eight possible destinations and complete launch-to-orbit insertion architectures constructed. Direct comparisons were made between aerocapture and competing orbit insertion techniques based on state-of-the-art and advanced chemical propulsion, solar electric propulsion, and aerobraking. The results show that three of the missions cannot be done without aerocapture: Neptune elliptical orbits, Saturn circular orbits, and Jupiter circular orbits. Aerocapture was found to substantially reduce the cost per unit mass delivered into orbit for five other missions based on a heavy launch vehicle: Venus circular orbits (55% reduction in \$/kg costs), Venus elliptical orbits (43% reduction); Mars circular orbits (13% reduction), Titan circular orbits (75% reduction), and Uranus circular orbits (69% reduction). These results were found to be relatively insensitive to 30% increases in both the estimated aerocapture system mass and system cost, suggesting that even modestly performing aerocapture systems will yield substantial mission benefits. Two other missions consisting of spacecraft in high eccentricity elliptical orbits at Mars and Jupiter were not shown to be improved by aerocapture. The last mission in the set consisting of an aeroassisted orbit transfer at Earth showed that aerocapture offered a 32% \$/kg reduction compared to chemical propulsion, but that aerobraking offered even better performance. Nevertheless, the problems of repeated passes through the Van Allen radiation belts are likely to preclude Earth aerobraking for most applications.

INTRODUCTION

Aerocapture is an orbit insertion maneuver in which a spacecraft flies through a planetary atmosphere and uses drag force to decelerate and effect a hyperbolic to elliptical orbit change. Although this kind of guided hypersonic flight is more complicated to execute than conventional chemical propulsion orbit insertion, the prospect of large propellant mass savings has served to motivate development of aerocapture technology over the past couple of decades.^{1,2,3,4} Sufficient technical maturity has now been obtained to support a flight test experiment in Earth orbit,⁵ with a clear infusion path for subsequent missions to Mars⁶ and Titan.⁷ It is expected that ongoing studies and research will produce similar technical maturity for aerocapture use at all other atmospheric worlds in the Solar System.⁸

The net mass advantage of aerocapture equals the difference between propulsion system mass and aerocapture system mass between the two approaches. The essential character of this comparison is best illustrated with a first order analysis in which the propulsion system mass is represented solely by the chemical propellant needed to effect the nominal orbit insertion velocity change (ΔV), and the aerocapture system mass is represented solely by the mass of the aeroshell required to protect the spacecraft and provide the required aerodynamic characteristics. The result is shown in Figure 1 where the before-to-after orbit insertion mass ratio of the spacecraft is plotted against the orbit insertion ΔV for the two approaches. The exponential curve for propulsion results directly from the rocket equation,

$$\frac{m_i}{m_f} = \exp\left(\frac{\Delta V}{I_{sp} g_0}\right) \quad (1)$$

* Senior Member, AIAA

where m_i and m_f are the initial and final masses of the spacecraft, respectively; ΔV is the change in velocity required for orbit insertion; I_{sp} is the specific impulse of the propulsion system; and g_0 is the gravitational constant, 9.81 m/s^2 . The quasi-linear aerocapture curve in Figure 1 is an estimate in which aeroshell mass fractions from past and present atmospheric entry missions are used as a proxy for aerocapture aeroshells at those planets listed in Table 1. Table 1 summarizes the quantitative data used in this approach, where the aeroshell mass fraction is the ratio of the aeroshell mass to the total vehicle mass, and the nominal aerocapture ΔV corresponds to insertion into a low circular orbit at the planet. If χ represents the aeroshell mass fraction in Table 1, then the conversion to mass ratio in Figure 1 follows from the simple algebraic equation:

$$\frac{m_i}{m_f} = \frac{1}{1 - \chi} \quad (2)$$

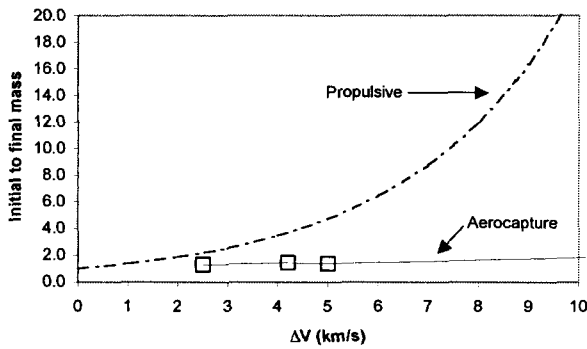


Figure 1. Comparison of Aerocapture to Propulsive Orbit Insertion Mass Ratios (Initial To Final)

Figure 1 clearly demonstrates the overwhelming mass advantage of aerocapture seen in the difference between the exponential curve and the quasi-linear curve. Even at the lowest ΔV of 2.5 km/s for Mars, aerocapture

offers an advantage of $M_i/M_f = 2.2 - 1.3 = 0.9$, which represents almost a doubling of the orbiting spacecraft mass (and presumably a doubling of the science value) or almost a halving of the launch vehicle requirement. Either result is of enormous benefit in a field where significant technology improvements are often measured in just a few kilograms.

Although the results in Figure 1 are instructive, it is desirable to both increase the fidelity of the mass benefit analysis and extend it to include financial cost considerations. It is important to realize that aerocapture is just one of several steps required to place a spacecraft into orbit around a planet, and those other steps can have a significant impact on the mass and cost advantages afforded by aerocapture. To cite one example, the use of a slower transfer ellipse to the outer Solar System will reduce the orbit insertion ΔV , and hence the aeroshell mass, at the cost of a longer trip time. The challenge of evaluating the trade-off between dissimilar attributes like smaller aeroshells versus longer trip times is one of the key motivators for adding monetary cost to the analysis. Although it is not the only metric for comparison, monetary cost does provide a quantitative measure that can be inclusive of the disparate elements required to place a spacecraft into a planetary orbit. One drawback to this approach is that monetary cost is an elusive variable. Historical and current costs are often viewed as proprietary information, and even when made available they are subject to questions about completeness and the existence of unusual circumstances that either inflated or decreased the actual cost. It is the premise of this study that, despite the inherent uncertainty in dealing with monetary costs, justifiable conclusions can be drawn about the benefits and cost-effectiveness of aerocapture. As shown below, the quantitative results are not very sensitive to changes in the assumed cost and mass metrics for aerocapture, thus supporting the premise.

Table 1. Historical Database for Aeroshell Mass Ratios

Entry Mission	Planet/Moon	Entry Date	Aeroshell Mass Fraction	Nominal Aerocapture ΔV for a Low Circular Orbit (km/s)
Pioneer-Venus (L)	Venus	1978	31%	4.2
Viking	Mars	1976	23%	2.5
Pathfinder	Mars	1997	21%	2.5
Galileo Probe	Jupiter	1995	60%	17.0
Huygens	Titan	2005	27%	5.0

The result of this approach is a spacecraft mass delivered into orbit combined with a monetary cost for doing so in each mission scenario. With multiple aerocapture and non-aerocapture scenarios at all feasible destinations, it becomes possible to quantify the benefits of aerocapture across the Solar System on both a mass and cost basis. The process also yields a \$/kg delivery cost metric that facilitates planet-to-planet comparisons.

AEROCAPTURE MISSION SET

Aerocapture can, in principle, be used at any of the eight worlds in the Solar System that have significant atmospheres. For each destination, there are an infinity of missions that can be performed corresponding to the infinity of possible orbits. Generally speaking, however, desirable spacecraft orbits tend to be of two kinds: low circular orbits suitable for planetary mapping and sample return missions, and high eccentricity elliptical orbits suitable for combined planet and natural satellite observations. Mars Global Surveyor is an example of the former, while Galileo is an example of the latter. For the purpose of representing the spectrum of aerocapture missions in this study, we have defined a set of eleven missions

across the eight destinations consisting of a circular orbit and/or an elliptical orbit at each world (Table 2). Note that some of these missions are taken directly from recent NASA strategic planning documents,⁹ while others represent less publicized missions or potentially unrecognized opportunities. It seems likely that some of these planetary missions will be NASA flagship missions, while others will be implemented through the competitive programs like NASA Discovery, Mars Scout, and New Frontiers. The Earth mission listed is a special case of an aeroassisted orbit transfer from geosynchronous transfer orbit to low Earth orbit. Although not strictly an aerocapture maneuver, this mission involves the same flight characteristics and is expected to be the basis of an Earth orbit flight test experiment of aerocapture technology. Potential applications include orbit transfer of secondary payloads launched to GTO and, in a small extrapolation, spacecraft returning from Lagrange points 4 and 5, the likely locations of future telescopes and space stations.

STUDY METHODOLOGY

Mass and cost calculations for the missions in Table 2 were performed on spreadsheets using a host of input

Table 2. Aerocapture Mission Set

Label	Destination	Mission Description	Nominal Inertial Entry Speed (km/s)	Nominal Orbit Insertion ΔV (km/s)
V1	Venus	Low circular orbit (300 km) for mapping and sample return	11.7	4.6
V2	Venus	8500 x 300 km elliptical orbit (e.g. Magellan)	11.7	3.3
E1	Earth	GTO to LEO aeroassisted transfer	10.3	2.3
M1	Mars	Low circular orbit (300 km) for mapping and sample return	5.9	2.4
M2	Mars	300 x 37,000 km elliptical orbit (e.g. Mars Odyssey pre-aerobraking)	5.9	1.2
J1	Jupiter	Low circular orbit (2000 km) inside the rings and radiation belt	59.0	17.0
J2	Jupiter	1000 x 1,880,000 km elliptical orbit (apoapsis at Callisto)	59.0	1.4
S1	Saturn	120,000 km circular orbit for ring observations in the Cassini gap	35.0	8.0
T1	Titan	1700 km circular orbit for mapping and aerobot/lander telecom relay	6.5	4.4
U1	Uranus	4,000 x 450,000 km elliptical orbit (apoapsis just beyond Titania)	24.0	4.5
N1	Neptune	4,000 x 430,000 km elliptical orbit (apoapsis just beyond Triton)	29.0	6.0

data, equations, and assumptions. Many cases were computed for each of the 11 missions consisting of a mixture of aerocapture and non-aerocapture scenarios so that direct comparisons could be made. The basic approach was to break down the mission architecture into a sequence of steps such that, given an injected mass capability of a particular launch vehicle, one could compute a delivered mass into the final working orbit at the destination. Note that in this study, delivered mass is the useful spacecraft mass remaining after the aeroshell and other associated aerocapture elements have been discarded. This process was roughly akin to a staging calculation in that vehicle mass was consumed or discarded at each step of the way. The cost of the various elements was also computed based on simplified parametric models so that an overall total delivery cost could be determined. Table 3 lists the steps in the calculation for both mass and cost. Implicit in each mission calculation is a separate interplanetary trajectory analysis that provided the required C_3 , trip time, and arrival velocity at the destination. Given that there are an infinity of possible trajectories for each mission, a single representative example was chosen after conducting a parametric study based on the common architectures.¹⁰

The numerical data used in the mass calculations is given in Table 4. Constant values with size are used for the chemical and solar electric propulsion (SEP) system dry mass-to-propellant mass ratios with the understanding they will be aggressive for very small systems and conservative for very large systems. The chemical propulsion system specifications are derived from historical data. The SEP system specifications are derived from a mixture of historical and projected systems. Specifically, the DS-1 NSTAR engine^{11,12,13} was used for the low power Venus and Mars scenarios, while all other trajectories used the next generation of ion thrusters, called NEXT.^{14,15,16} The NSTAR engine is a 2.3 kW, 30-cm diameter engine with a maximum specific impulse (I_{sp}) of 3100 s and 130 kg of throughput per engine, while the NEXT engine is a 6.2 kW, 40-cm diameter engine with a maximum I_{sp} of 4000 s and 250 kg of throughput per engine. The solar array for the SEP system assumed a specific mass of 130 kg/kW for the 5-10 kW class trajectories and 150 kg/kW for the 25 kW class trajectories. The SEP system dry mass fraction also assumes 30% contingency on the dry mass and 10% contingency on the propellant mass. It is representative of a complete SEP module design and thus includes all the structure, cabling, thermal, power, attitude control,

Table 3. Computation Methodology for Mass and Cost

	Element Description	Mass Calculation	Cost Calculation
1	Launch from Earth at a specified C_3	Use NASA data for injected mass capability at specified C_3 ¹⁰ ; choose between small (Delta 2925), medium (Delta 4450, Atlas 551) and large (Delta 4050H) launchers	Use NASA provided data on estimated cost of the specified launch vehicle
2	Use of in-space propulsion	Rocket equation to compute propellant usage based on required ΔV ; rules of thumb to estimate propulsion system dry mass and mass of supporting structure	Parametric cost curves based on propulsion system dry mass
3	Gravity assist maneuver(s)	Propellant mass for targeting maneuvers accounted for in Step 2.	No cost allocated, but trip time is accounted in Step 4
4	In space cruise	No mass allocated	Estimated cost per month for operations and ground support
5	Orbit insertion with propulsion	Rocket equation to compute propellant usage; rules of thumb to estimate propulsion system dry mass and mass of supporting structure	Parametric cost curves based on propulsion system dry mass
6	Aerobraking or Aerocapture	No mass required for aerobraking; aerocapture mass fraction estimated from historical entry vehicle aeroshells (Fig. 1, Table 4)	Aerobraking: parametric cost curve based on vehicle mass; Aerocapture: parametric cost curve based on vehicle mass
7	Post-aerocapture periapse raise maneuver	Rocket equation to compute propellant usage; rules of thumb to estimate propulsion system dry mass and mass of supporting structure	Parametric cost curves based on propulsion system dry mass

feed system, tanks, thrusters, driving electronics, and redundancy that goes along with it.

The aerocapture system mass fractions in Table 4 are estimates derived from the simple performance curve in Figure 1 with approximately 0.05 added in each case to account for uncertainties and extra non-aeroshell components required for aerocapture. Examples of extra non-aeroshell aerocapture components include heat transfer equipment for thermal control of radioisotope thermo-electric generators (RTGs) inside the aeroshell and telecommunications antennas that are discarded prior to atmospheric entry. Detailed systems analyses have provided aerocapture mass fraction values for Earth⁵ and Titan⁷ which are consistent with this simplified approach. Note the implicit simplification that a fixed aerocapture mass fraction can be used at each planet even though different interplanetary trajectories will have slightly different entry velocities.

Table 4. Numerical Values Used in Mass Computations

Element	Value
Chemical propulsion module: dry mass / propellant mass	0.2
Solar electric propulsion module: dry mass / propellant mass	1.55
Stack support structural mass / propulsion module mass	0.05
State-of-the-art storable chemical propellant I_{sp}	325 s
Future advance storable chemical propellant I_{sp} ¹⁷	370 s
Solar electric propulsion specific impulse ¹⁸	4000 s
Aerocapture system mass fraction: Venus	0.30
Aerocapture system mass fraction: Earth	0.30
Aerocapture system mass fraction: Mars	0.25
Aerocapture system mass fraction: Jupiter	0.65
Aerocapture system mass fraction: Saturn	0.55
Aerocapture system mass fraction: Titan	0.35
Aerocapture system mass fraction: Uranus	0.45
Aerocapture system mass fraction: Neptune	0.45

The cost input data summarized in Table 5 is comprised of a mixture of well-defined publicized costs, published and unpublished studies, anecdotal evidence and educated guesses. Note that no attempt has been made to include the effects of monetary inflation in this analysis, so that the costs in Table 5 are essentially current year (2003) costs. Fixed values are used for the launch vehicles, a per month cost for operations and ground support during in-space cruise, and square root parametric costs as a function of mass for the other elements; i.e., in-space propulsion, propulsion module-to-aeroshell interface structure, aerobraking, and aerocapture. Aerobraking costs are also linearly scaled with the ΔV required for orbit circularization. The use of a square root function to represent the cost versus mass relationship is a simplification that is intended to capture the essential feature that larger systems cost more but that economies of scale limit that growth to a less-than-linear dependence. Where possible, these square root cost curves have been anchored to at least one data point from either a historical mission or recent detailed studies (References 20 to 23). These square root cost functions are plotted in Figure 2.

RESULTS AND DISCUSSION

This study generated a very large amount of data, only a fraction of which can be included due to space constraints. Figures 3a-3j show plots of delivered mass versus delivery cost for all 10 non-Earth missions listed in Table 2. The eleventh mission, aeroassisted orbit transfer at Earth, will be treated separately at the end of the section. Each figure is a scatter plot comprised of multiple scenarios where the symbols are used to denote the method of orbit insertion:

- filled diamonds for state of the art chemical propulsion with an $I_{sp} = 325$ s
- open diamonds for advanced chemical propulsion with an $I_{sp} = 370$ s
- stars for aerobraking
- filled circles for aerocapture
- filled squares for solar electric propulsion
- negative mass values in the plots denote not-feasible scenarios.

Tables 6 through 8 provide the raw data for each computed scenario, listing the trip time, delivered mass and delivered cost, respectively. In these tables, “V/E” denotes one or more Venus and/or Earth gravity assist, “J” denotes a Jupiter gravity assist, “chem325” and “chem370” denote chemical propulsion with either a 325 or 370 s specific impulse, “A/B” denotes

Table 5. Numerical Values Used in Cost Computations

Element	Cost = a + bx ^{0.5}				Source/Justification
	a	b	x	units	
Delta 2925	102	N/A	N/A	\$M	Ref. ¹⁹
Delta 4450	145	N/A	N/A	\$M	Ref. ¹⁹
Delta 4050H	190	N/A	N/A	\$M	Ref. ¹³
Cruise operations cost	18	N/A	N/A	\$M / year	Author's estimate (includes low level science team support)
SOA chemical propulsion	2	1.7	dry mass of prop system (kg)	\$M	Ref. ²⁰
Advanced chemical propulsion	3	2.25	dry mass of prop system (kg)	\$M	Author's estimate that advanced chemical will be 50% more costly than SOA chemical
Solar electric propulsion	40	0.8	dry mass of prop system (kg)	\$M	Ref. ²¹
Aeroshell – prop. module interface structure	2	0.5	interface structure mass (kg)	\$M	Author's estimate
Aerobraking mass function	5	0.2	mass of delivered spacecraft (kg)	\$M	Ref. ²²
Aerobraking ΔV coefficient	ΔV/1.2	N/A	mass of delivered spacecraft (kg)	N/A	Assumes cost linearly scales with ΔV
Aerocapture	7	0.8	mass of aeroshell (kg)	\$M	Ref. ²²

aerobraking, “A/C” denotes aerocapture and SEP denotes solar electric propulsion. 19 20 21 22 23

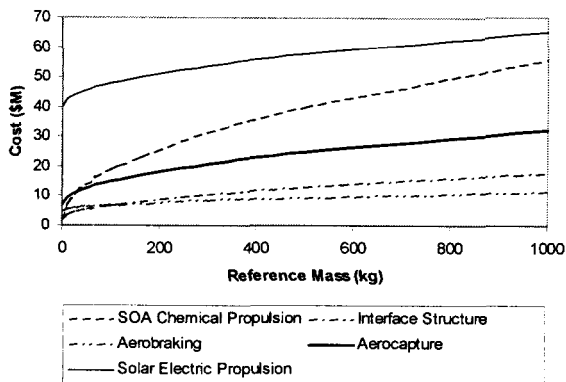


Figure 2. Square Root Cost Functions

There are several noteworthy results illustrated in Figure 3. Perhaps the most important is that the aerocapture data points (filled circles) generally lie to the right of the non-aerocapture points, thus confirming the expectation (Figure 1) that aerocapture possesses a mass advantage over other orbit insertion techniques. This advantage is small when the orbit insertion

velocity change is small (e.g., Mission M1, ΔV = 2.4 km/s) and it is large when the orbit insertion velocity change is large (e.g., Mission N1, ΔV = 5-7 km/s). Note that the Jupiter low circular orbit mission (J1) and the Saturn Ring Observer Mission (S1) are so challenging that they do not show any non-aerocapture scenarios with a positive delivered mass. For these missions aerocapture is truly enabling, a description that can also be applied to the Neptune Orbiter mission (N1) since the maximum non-aerocapture delivered mass of 180 kg (Scenario 35) is too small for a practical orbiter unless highly capable microspacecraft become available. In contrast, the Mars high eccentricity mission (M2) shows essentially no benefit with aerocapture and the Jupiter high eccentricity orbit mission (J2) shows that aerocapture actually delivers less mass than competing architectures. The explanation for Jupiter is that the high entry velocities require large aeroshell mass fractions (~65%) to protect the spacecraft, but this mass cannot be recouped in propellant saving because the orbit insertion ΔV is only ~1.4 km/s. The same logic applies to Mission M2 although in this case the propellant savings are equal to the aerocapture system mass so that no advantage or disadvantage results. For all other missions shown in Figure 3 and Table 7, aerocapture improves, and often

Table 6. Trip Times for All Mission Scenarios

No.	Launch Vehicle	Transit Propulsion	Gravity Assist	Orbit Insertion	Mission and Trip Time (years)											
					V1	V2	M1	M2	J1	J2	S1	T1	U1	N1		
1	Delta 2925	None	None	chem325	0.5	0.5	0.8	0.8								
2	Delta 2925	None	None	chem370	0.5	0.5	0.8	0.8								
3	Delta 2925	None	None	A/B	0.5	0.5	0.8	0.8								
4	Delta 2925	None	None	A/C	0.5	0.5	0.8	0.8								
5	Delta 4450	None	None	chem325	0.5	0.5	0.8	0.8								
6	Delta 4450	None	None	chem370	0.5	0.5	0.8	0.8								
7	Delta 4450	None	None	A/B	0.5	0.5	0.8	0.8								
8	Delta 4450	None	None	A/C	0.5	0.5	0.8	0.8								
9	Delta 4450	chem325	V/E	chem325					6.1	6.1	7.5	7.5				
10	Delta 4450	chem370	V/E	chem370					6.1	6.1	7.5	7.5				
11	Delta 4450	chem325	V/E	A/C					6.1	6.1	7.5	7.5				
12	Delta 4450	chem325	V/E + J	chem325											9.0	10.7
13	Delta 4450	chem325	V/E + J	chem370											9.0	10.7
14	Delta 4450	chem325	V/E + J	A/C											9.0	10.7
15	Delta 4450	SEP	V/E	chem325					3.5	3.5	6.0	6.0	8.0	10.5		
16	Delta 4450	SEP	V/E	chem370					3.5	3.5	6.0	6.0	8.0	10.5		
17	Delta 4450	SEP	V/E	A/C					3.5	3.5	6.0	6.0	8.0	10.5		
18	Delta 4450	SEP	V/E + J	chem325							6.7	6.7	8.4			
19	Delta 4450	SEP	V/E + J	chem370							6.7	6.7	8.4			
20	Delta 4450	SEP	V/E + J	A/C							6.7	6.7	8.4			
21	Atlas 551	SEP	V/E + J	chem325												10.5
22	Atlas 551	SEP	V/E + J	chem370												10.5
23	Atlas 551	SEP	V/E + J	A/C												10.5
24	Delta 4050H	None	None	chem325	0.5	0.5	0.8	0.8	2.2	2.2				9.0		
25	Delta 4050H	None	None	chem370	0.5	0.5	0.8	0.8	2.2	2.2				9.0		
26	Delta 4050H	None	None	A/B	0.5	0.5	0.8	0.8								
27	Delta 4050H	None	None	A/C	0.5	0.5	0.8	0.8	2.2	2.2				9.0		
28	Delta 4050H	chem325	V/E	chem325					6.1	6.1	7.5	7.1				
29	Delta 4050H	chem370	V/E	chem370					6.1	6.1	7.5	7.1				
30	Delta 4050H	chem325	V/E	A/C					6.1	6.1	7.5	7.1				
31	Delta 4050H	chem325	V/E + J	chem325							7.7	6.7	9.0	10.7		
32	Delta 4050H	chem370	V/E + J	chem370							7.7	6.7	9.0	10.7		
33	Delta 4050H	chem325	V/E + J	A/C							7.7	6.7	9.0	10.7		
34	Delta 4050H	SEP	V/E	chem325					4.0	4.0	6.0	6.0	8.0	10.5		
35	Delta 4050H	SEP	V/E	chem370					4.0	4.0	6.0	6.0	8.0	10.5		
36	Delta 4050H	SEP	V/E	A/C					4.0	4.0	6.0	6.0	8.0	10.5		
37	Delta 4050H	SEP	V/E + J	chem325							6.7	6.7	8.4	10.5		
38	Delta 4050H	SEP	V/E + J	chem370							6.7	6.7	8.4	10.5		
39	Delta 4050H	SEP	V/E + J	A/C							6.7	6.7	8.4	10.5		
40	Delta 4050H	SEP	None	SEP	2.5	2.2	1.4	1.4								
41	Delta 4450	SEP	None	SEP	2.4	2.1	1.5	1.3								
42	Delta 2925	SEP	None	SEP	2.5	2.2	1.3	1.2								

Table 7. Delivered Mass for All Mission Scenarios

No.	Launch Vehicle	Transit Propulsion	Gravity Assist	Orbit Insertion	Mission and Delivered Mass (kg)											
					V1	V2	M1	M2	J1	J2	S1	T1	U1	N1		
1	Delta 2925	None	None	chem325	105	275	432	729								
2	Delta 2925	None	None	chem370	171	344	495	774								
3	Delta 2925	None	None	A/B	265	275	702	729								
4	Delta 2925	None	None	A/C	788	788	807	807								
5	Delta 4450	None	None	chem325	318	835	1309	2210								
6	Delta 4450	None	None	chem370	519	1046	1499	2344								
7	Delta 4450	None	None	A/B	804	835	2128	2210								
8	Delta 4450	None	None	A/C	2395	2395	2444	2444								
9	Delta 4450	chem325	V/E	chem325					-652	2007	-130	208				
10	Delta 4450	chem370	V/E	chem370					-634	2143	-93	304				
11	Delta 4450	chem325	V/E	A/C					1048	1048	129	762				
12	Delta 4450	chem325	V/E + J	chem325											166	-98
13	Delta 4450	chem325	V/E + J	chem370											287	-45
14	Delta 4450	chem325	V/E + J	A/C											912	681
15	Delta 4450	SEP	V/E	chem325					-385	1089	-200	231	294	42		
16	Delta 4450	SEP	V/E	chem370					-374	1176	-143	330	378	93		
17	Delta 4450	SEP	V/E	A/C					619	619	179	1059	748	481		
18	Delta 4450	SEP	V/E + J	chem325							-260	127	239			
19	Delta 4450	SEP	V/E + J	chem370							-192	242	349			
20	Delta 4450	SEP	V/E + J	A/C							222	1315	1005			
21	Atlas 551	SEP	V/E + J	chem325												-52
22	Atlas 551	SEP	V/E + J	chem370												32
23	Atlas 551	SEP	V/E + J	A/C												901
24	Delta 4050H	None	None	chem325	675	1770	2802	4693	-454	1339				103		
25	Delta 4050H	None	None	chem370	1101	2218	3208	4983	-441	1438				340		
26	Delta 4050H	None	None	A/B	1705	1770	4556	4693								
27	Delta 4050H	None	None	A/C	5078	5078	5232	5232	729	729				113		
28	Delta 4050H	chem325	V/E	chem325					-1407	4334	-294	472				
29	Delta 4050H	chem370	V/E	chem370					-1369	4628	-211	691				
30	Delta 4050H	chem325	V/E	A/C					2262	2262	292	1731				
31	Delta 4050H	chem325	V/E + J	chem325							-485	253	357	-222		
32	Delta 4050H	chem370	V/E + J	chem370							-353	502	618	-102		
33	Delta 4050H	chem325	V/E + J	A/C							494	2630	1966	1543		
34	Delta 4050H	SEP	V/E	chem325					-579	1709	-311	278	115	113		
35	Delta 4050H	SEP	V/E	chem370					-563	1835	-222	429	237	180		
36	Delta 4050H	SEP	V/E	A/C					930	930	278	1645	1175	601		
37	Delta 4050H	SEP	V/E + J	chem325							-439	244	179	-78		
38	Delta 4050H	SEP	V/E + J	chem370							-323	441	366	81		
39	Delta 4050H	SEP	V/E + J	A/C							375	2218	1819	1680		
40	Delta 4050H	SEP	None	SEP	2834	3542	3471	4222								
41	Delta 4450	SEP	None	SEP	1412	1760	2168	2607								
42	Delta 2925	SEP	None	SEP	221	366	508	660								

Table 8. Total Delivery Cost for All Mission Scenarios

No.	Launch Vehicle	Transit Propulsion	Gravity Assist	Orbit Insertion	Mission and Delivery Cost (\$M)											
					V1	V2	M1	M2	J1	J2	S1	T1	U1	N1		
1	Delta 2925	None	None	chem325	136	134	137	133								
2	Delta 2925	None	None	chem370	147	143	147	140								
3	Delta 2925	None	None	A/B	142	134	143	133								
4	Delta 2925	None	None	A/C	140	140	145	149								
5	Delta 4450	None	None	chem325	196	193	194	187								
6	Delta 4450	None	None	chem370	215	210	210	198								
7	Delta 4450	None	None	A/B	203	193	201	187								
8	Delta 4450	None	None	A/C	199	199	202	208								
9	Delta 4450	chem325	V/E	chem325					303	284	322	320				
10	Delta 4450	chem370	V/E	chem370					326	296	340	336				
11	Delta 4450	chem325	V/E	A/C					311	311	343	335				
12	Delta 4450	chem325	V/E + J	chem325											354	379
13	Delta 4450	chem325	V/E + J	chem370											374	397
14	Delta 4450	chem325	V/E + J	A/C											373	395
15	Delta 4450	SEP	V/E	chem325					319	306	358	355	388	433		
16	Delta 4450	SEP	V/E	chem370					337	316	374	368	399	444		
17	Delta 4450	SEP	V/E	A/C					327	327	377	361	397	441		
18	Delta 4450	SEP	V/E + J	chem325							373	371	398			
19	Delta 4450	SEP	V/E + J	chem370							391	386	412			
20	Delta 4450	SEP	V/E + J	A/C							393	375	406			
21	Atlas 551	SEP	V/E + J	chem325												436
22	Atlas 551	SEP	V/E + J	chem370												451
23	Atlas 551	SEP	V/E + J	A/C												443
24	Delta 4050H	None	None	chem325	259	255	254	244	270	256					425	
25	Delta 4050H	None	None	chem370	287	280	276	260	289	266					454	
26	Delta 4050H	None	None	A/B	268	255	261	244								
27	Delta 4050H	None	None	A/C	260	260	263	263	278	278					440	
28	Delta 4050H	chem325	V/E	chem325					368	341	387	376				
29	Delta 4050H	chem370	V/E	chem370					401	358	413	399				
30	Delta 4050H	chem325	V/E	A/C					377	377	414	395				
31	Delta 4050H	chem325	V/E + J	chem325							391	370	420	444		
32	Delta 4050H	chem370	V/E + J	chem370							418	394	447	469		
33	Delta 4050H	chem325	V/E + J	A/C							419	384	444	463		
34	Delta 4050H	SEP	V/E	chem325					383	366	415	411	447	490		
35	Delta 4050H	SEP	V/E	chem370					404	378	434	427	463	501		
36	Delta 4050H	SEP	V/E	A/C					391	391	436	416	454	498		
37	Delta 4050H	SEP	V/E + J	chem325							434	430	461	500		
38	Delta 4050H	SEP	V/E + J	chem370							456	449	480	520		
39	Delta 4050H	SEP	V/E + J	A/C							457	434	468	507		
40	Delta 4050H	SEP	None	SEP	325	318	292	288								
41	Delta 4450	SEP	None	SEP	263	257	240	233								
42	Delta 2925	SEP	None	SEP	210	204	183	180								

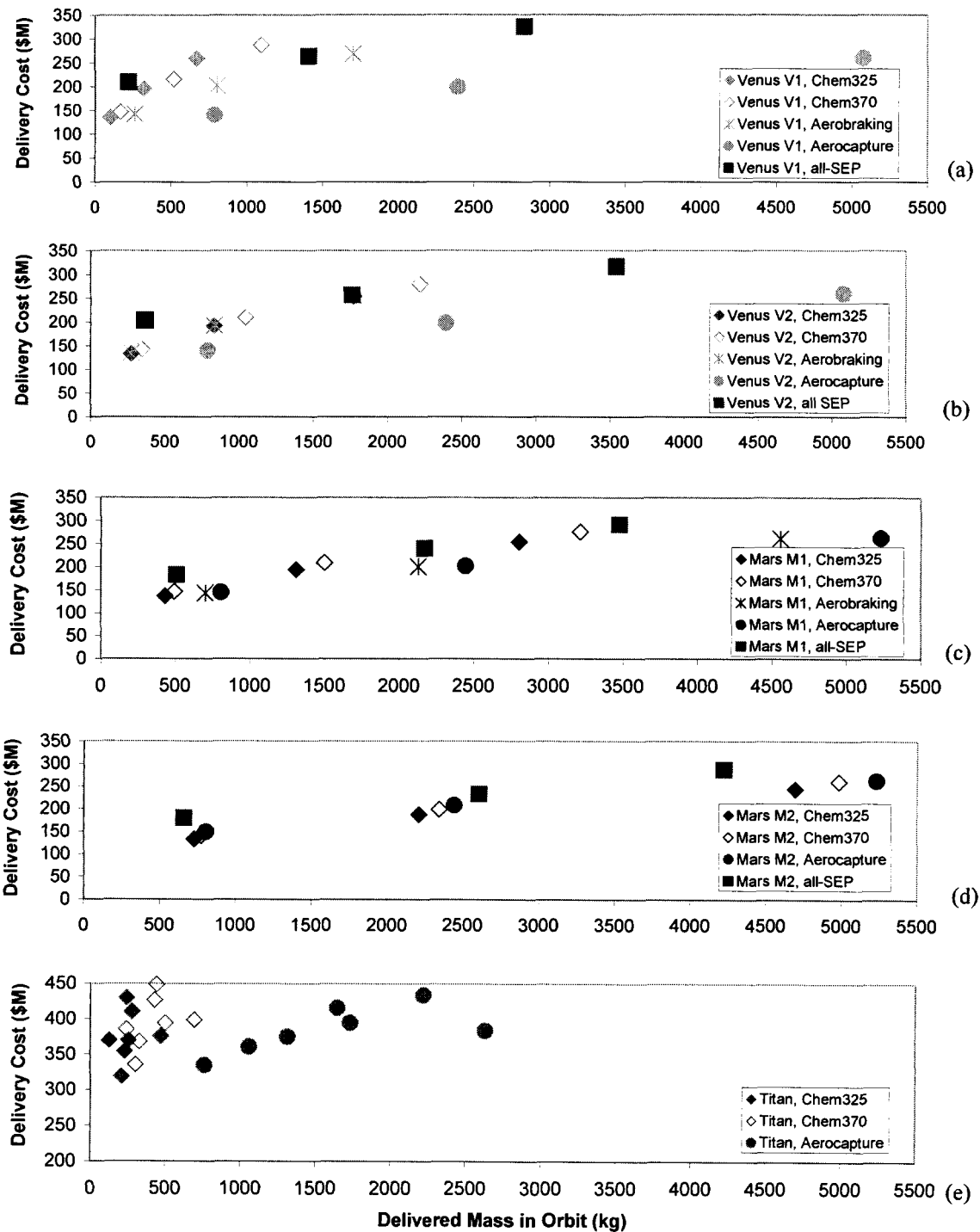


Figure 3. Delivered Mass vs. Delivery Cost for All Non-Earth Missions

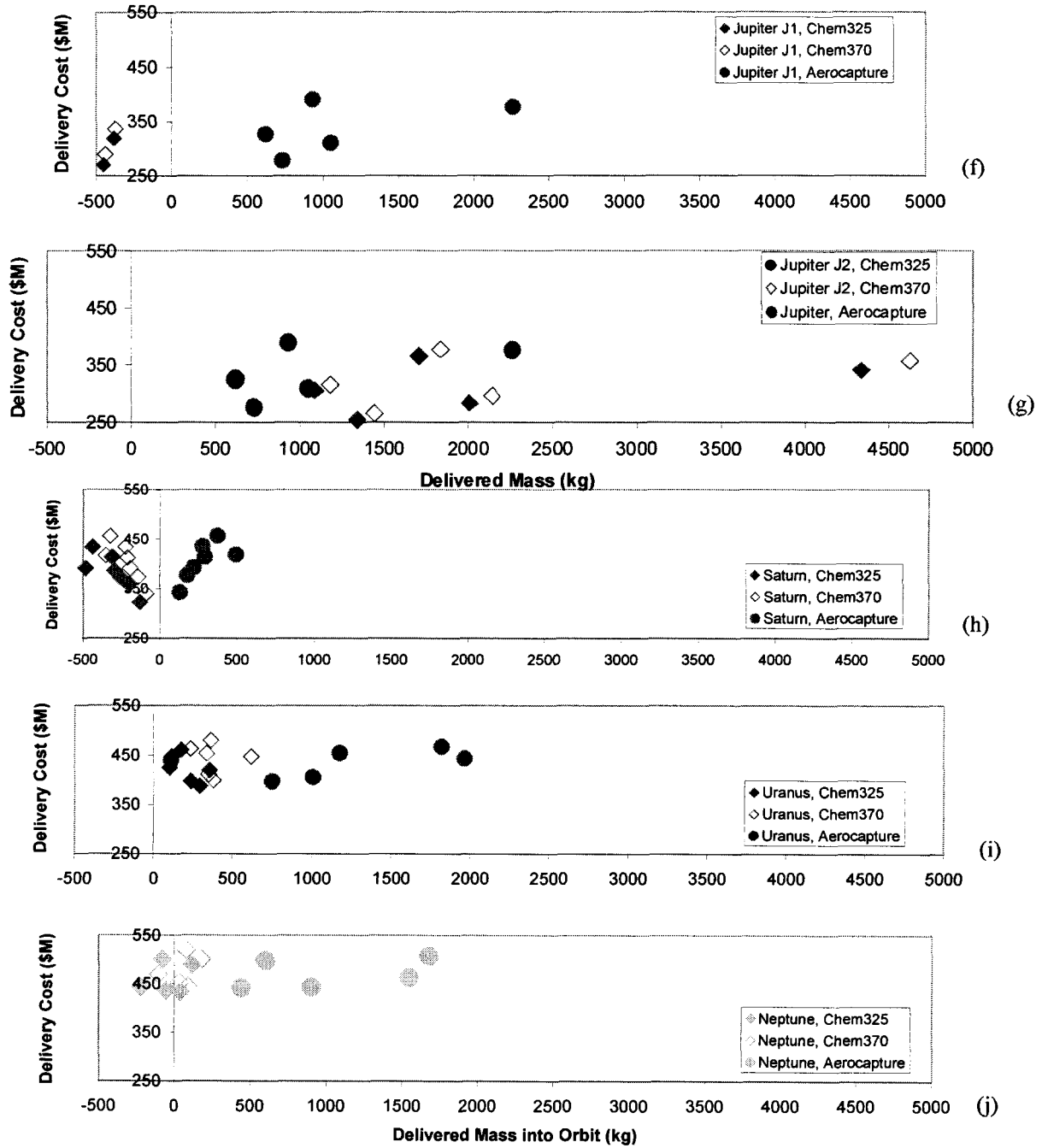


Figure 3. Delivered Mass vs. Delivery Cost for All Non-Earth Missions (Continued)

substantially improves, the ability to deliver mass into the desired orbit. To highlight just one example, the Titan Orbiter Scenario 33 provides a factor of 3.8 improvement in delivered mass versus the best competition Scenario 29 (2630 kg vs. 691 kg). Note that if the delivered mass requirements for Titan and Uranus are sufficiently large (approximately >600 kg) then aerocapture becomes an enabling technology for them based on the mass limit of the Delta IV heavy launch vehicle. Another notable result is that the use of solar electric propulsion to achieve orbit at Venus and Mars shows worse performance than aerocapture, despite the relatively high solar flux and extraordinary specific impulse of SEP thrusters. This is due to a combination of the high dry mass inherent to SEP designs and the significant gravity losses associated with long duration spiral trajectories into orbit.

It is interesting to note that the cost data do not show such dramatic many-fold improvements by using aerocapture. The reason is that the orbit insertion costs are just a small fraction (10-20%) of the overall delivery costs because of the dominating effect of launch vehicle, multi-year operations and (where applicable) in-space chemical or solar electric propulsion module costs. Moreover, the projected cost of aerocapture systems are comparable to the cost of chemical propulsion systems for orbit insertion, so that any aerocapture advantage generally results from shorter trip times or smaller launch vehicles, advantages that cannot produce large cost reductions on a percentage basis. Nevertheless, in absolute terms the savings of a few tens of millions of dollars can be

critical to the success of competed missions in a cost-constrained environment. For example, a roughly 700 kg Titan orbiter can be delivered for \$399M without aerocapture (Scenario 26) or \$335M with aerocapture (Scenario 11), where the \$64M savings (16%) result from using a medium rather than a heavy launch vehicle. Another notable result seen in the data is that each mission has a minimum delivery cost corresponding to the smallest available launch vehicle, one that is mostly independent of the orbit insertion technique. These minimum costs range from approximately \$140M for Venus and Mars, to \$320M for Saturn and Titan, to \$380M for Neptune. Note that these minimum costs correspond to conventional orbiter sizes of several hundred kilograms and therefore do not apply to much smaller micro-spacecraft.

Table 9 presents a \$/kg metric for each mission using the best aerocapture and best non-aerocapture scenarios in both the medium and heavy launch vehicle categories. The data for the medium launch vehicle is also plotted in Figure 4. It can be seen in Table 9 that although the economy of scale produces lower \$/kg costs for the heavy launch vehicle, the percentage improvement offered by aerocapture technology is largely independent of the launch vehicle size. This percentage improvement is substantial for the seven missions (V1, V2, J1, S1, T1, U1 and N1) with a large orbit insertion ΔV requirement, ranging from a 43% to 100% reduction of cost per unit mass. In this context, a 100% improvement corresponds to a mission that cannot be done without aerocapture. The high eccentricity Mars (M2) and Jupiter (J2) missions are not

Table 9. Summary of \$M/kg Metrics for All Missions

	Medium Launch Vehicle				Heavy Launch Vehicle			
	Best A/C	Best non-A/C	% Improvement	What is best non-A/C?	Best A/C	Best non-A/C	% Improvement	What is best non-A/C?
Venus V1	0.08	0.19	56%	all-SEP	0.05	0.11	55%	all-SEP
Venus V2	0.08	0.15	43%	all-SEP	0.05	0.09	43%	all-SEP
Mars M1	0.08	0.09	12%	A/B	0.05	0.06	13%	A/B
Mars M2	0.09	0.08	-1%	chem325	0.05	0.05	3%	chem325
Jupiter J1	0.30	1000.00	100%	N/A	0.17	1000.00	100%	N/A
Jupiter J2	0.30	0.14	-115%	chem370	0.17	0.08	-115%	chem370
Saturn S1	1.77	1000.00	100%	N/A	0.85	1000.00	100%	N/A
Titan T1	0.29	1.10	74%	chem370	0.15	0.58	75%	chem370
Uranus U1	0.40	1.06	62%	chem370	0.23	0.72	69%	chem370
Neptune N1	0.49	4.79	90%	chem370	0.30	2.78	89%	chem370

helped by aerocapture, as discussed above, while the low circular orbit M1 mission shows a modest improvement of 12%.

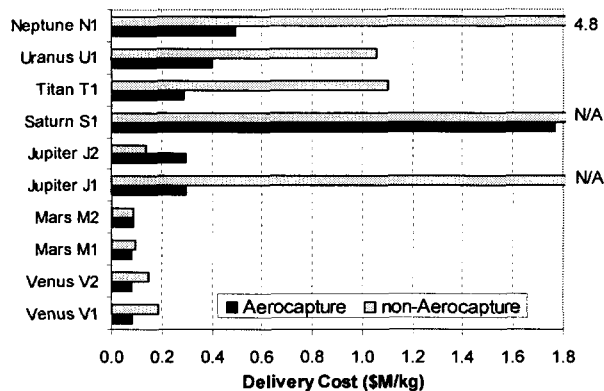


Figure 4. Best Scenario Delivery Costs Per Unit Mass for a Medium Launch Vehicle

One way to put the magnitude of the aerocapture performance improvements into perspective is to compute the equivalent propulsion system specific impulse that would be required to match the aerocapture delivered mass with a non-aerocapture approach. The results are shown in Table 10 where, except for M2 and J2 missions that are not helped by aerocapture, the required specific impulse exceeds any available or planned storable chemical propulsion system. Note that the relatively low required specific impulse for the Saturn Ring Observer mission reflects the fact that it requires a large 3.3 km/s periapse raise maneuver to circularize the orbit in the Cassini gap of the rings, and therefore direct propulsive orbit insertion with a much improved specific impulse will save all of the propellant associated with this large maneuver.

Table 10. Required Specific Impulse to Match Aerocapture Performance

Mission	Required Equivalent Isp (s)
Venus V1	1060
Venus V2	970
Mars M1	455
Mars M2	-
Jupiter J1	2040
Jupiter J2	-
Saturn S1	640
Titan T1	1240
Uranus U1	815
Neptune N1	1140

The performance advantages of aerocapture for most of the missions in this set are so large that they are not significantly compromised by large increases in the predicted aerocapture system mass fraction or cost. Table 11 shows the results of a sensitivity study based on medium launch vehicles in which either the aerocapture system mass or the aerocapture system cost were increased by 30% while holding all other parameters constant. The change in the percentage advantage of aerocapture on a \$/kg delivery basis is small in all cases except for the M1 mission where a mass increase of this size eliminates the modest aerocapture advantage. Note also that the increased mass effect always causes a greater change than increased cost, which is just a reflection of the fact that aerocapture costs are only a small fraction of the overall delivery cost. The conclusion is that most of the projected aerocapture advantage on a \$/kg delivery basis will be retained even in the event that the mass or cost of aerocapture technology is 30% greater than expected. Conversely, improvements resulting from superior-than-expected aerocapture mass or cost performance will also be small on a percentage basis; however, on a net basis, the potential savings of many millions of dollars should still serve as a powerful motivator for producing efficient aerocapture systems.

Table 11. Sensitivity of the Aerocapture Advantage (Medium Launch Vehicle Scenarios)

Mission	Aerocapture Advantage		
	Nominal Case	+30% A/C mass	+30% A/C cost
Venus V1	56%	49%	53%
Venus V2	43%	35%	40%
Mars M1	12%	1%	8%
Mars M2	-	-	-
Jupiter J1	100%	100%	100%
Jupiter J2	-	-	-
Saturn S1	100%	100%	100%
Titan T1	74%	69%	74%
Uranus U1	62%	49%	61%
Neptune N1	90%	86%	90%

Based on the planetary results presented above, it is possible to categorize the aerocapture missions into three groups: enabled (J1, S1, N1), improved (V1, V2, M1, T1, U1) and not helped (M2, J2). For the improved category, the aerocapture benefit can manifest itself in a reduced delivery cost, an increased spacecraft mass, or a combination of the two. The preferred optimization will necessarily depend on the

details of any given mission, but results for the two limits are presented in Tables 12 and 13. For the fixed cost limit in Table 12, the heavy launch vehicle mass and cost data is used for each of the five missions to produce a net delivered mass increase. This mass increase is equivalent to the horizontal distance between the aerocapture and non-aerocapture data points on the appropriate mission plots in Figure 3. Similarly, the fixed mass limit can be obtained by measuring the vertical distance between the aerocapture and non-aerocapture data points in Figure 3, which for the Venus and Mars missions happens to correspond to the difference between the \$/kg cost of aerocapture with a medium launch vehicle and the best non-aerocapture cost on a heavy launch vehicle (see Table 13). However, this method breaks down with the Titan and Uranus missions because there are not any non-aerocapture scenarios that can deliver as much mass as the most efficient aerocapture scenarios based on a medium launch vehicle. Therefore, we have estimated a \$/kg cost of a hypothetical ultra heavy launch vehicle that could deliver sufficient mass in the T1 and U1 non-aerocapture scenarios. Note that these delivery costs must reflect economies of scale and therefore are significantly better than those based on existing heavy vehicles; however, they do not include the sizable research and development costs associated with any new launch vehicle. With these caveats, it can be seen that only four of the five missions show a cost savings, with values ranging from \$28M for the Venus V2 mission to \$97M for the Titan mission. The Mars M1 mission does not show a cost savings because the size scaling dilution effect is larger than the aerocapture performance benefit. This suggests that the use of aerocapture at Mars will not be primarily for cost reduction but rather for increasing the spacecraft mass for a fixed delivery system as shown in Table 12.

One important caveat to this conclusion is that Mars missions are amenable to co-manifesting, that is sending two spacecraft using a single large launch vehicle rather than two smaller launch vehicles. For example, aerocapture would allow a single Delta IV heavy to send a pair of 2500 kg spacecraft to Mars (Mission M1, Scenario 27, capability = 5232 kg), but aerobraking would not (Mission M1, Scenario 26, capability = 4556 kg). The use of one Delta IV heavy versus two Delta IV mediums would result in a launch vehicle cost savings of \$100M, a result not represented in the methodology of Table 13. The original CNES plan for the 2005/2007 Mars Sample Return Mission in fact proposed exactly this approach with the lander and the sample return orbiter launched on a single Ariane-5.

A second important caveat for Mars is that if the time delay of multi-month aerobraking into orbit is not acceptable (e.g., if the orbiter must support landed assets immediately or if astronauts are on board) then the aerocapture performance advantage for the Mars M1 mission becomes much larger, increasing from 12% to 41% versus the next best option of advanced chemical (chem370) propulsive orbit insertion.

Table 12. Projected Spacecraft Mass Increases for Aerocapture Improved Missions

Mission	Non-A/C \$/kg for Heavy Launcher	A/C \$/kg for Heavy Launcher	Delivery Cost (\$M)	Mass increase per spacecraft (kg)
V1	0.11	0.05	260	2804
V2	0.09	0.05	260	2174
M1	0.06	0.05	260	649
T1	0.58	0.15	390	1997
U1	0.69	0.23	430	1281

Table 13. Projected Cost Savings for Aerocapture Improved Missions

Mission	Non-A/C \$/kg for Heavy Launcher	A/C \$/kg for Medium Launcher	Spacecraft Mass (kg)	Cost savings per spacecraft (\$M)
V1	0.11	0.08	2400	76
V2	0.09	0.08	2400	16
M1	0.06	0.08	2400	-61
T1*	0.36	0.29	1300	97
U1*	0.49	0.40	1000	86

* Estimated \$/kg value for an hypothetical ultra-heavy launch vehicle that can deliver the listed spacecraft mass.

From a technology development point of view, it is desirable to estimate the total return on investment. Although aerocapture technology has considerable maturity, it is generally accepted that a flight test experiment will be required before aerocapture will be used on any NASA science mission. Additionally, some level of modeling and ground-based experimentation will be required for the more challenging gas giant planet missions, particularly in the areas of aerothermodynamics and thermal

protection systems. Based on the work in References 5 and 8, it is estimated that the combination of flight test and gas giant planet development will require an investment on the order of \$100M. According to the methodology used to generate Table 13, an investment of this magnitude will be returned almost completely in a single V1, T1 or U1 mission. The investment returns for the V2 and M1 missions are not significant from the pure cost savings perspective, although the mass improvement shown in Table 12 may justify a \$100M investment in itself. It is difficult to quantify the return on investment for the enabled missions to Jupiter, Saturn, and Neptune because there are no existing non-aerocapture alternatives that can be used as reference points. One possible approach is to use a new technology that is under development, namely nuclear electric propulsion (NEP) based on 100 kW class fission reactors. In principle, this technology will be able to do the J1, S1, and N1 missions with the added benefit of abundant electrical power once in orbit. However, the per unit cost after completion of technology development is projected to be on the order of a billion dollars, a cost that far exceeds any of the aerocapture-based mission architectures. Therefore, it seems justified to conclude that aerocapture technology will provide at least an order of magnitude return on a \$100M investment after just the first use on an enabled mission.

The methodology for analyzing the Earth mission E1 was different than the others because the assumed initial condition of a GTO orbit precludes consideration of the launch vehicle and in-space trajectory. Therefore, only Steps 6 and 7 in Table 3 were involved in the computation. The results are shown in Figure 5 where the size scaling is illustrated by simply computing arbitrary initial masses of 300, 1000, and 3000 kg. Not surprisingly, the aerobraking scenarios show a clear performance advantage at all scales. This results from the fact that aerobraking requires essentially no mass and, in this case, the usual precursor step of propulsive insertion into a high eccentricity orbit

is not involved. The data also show that the operations cost of aerobraking is approximately the same as an aerocapture system, so there is no net cost advantage either way. On a \$/kg basis, aerocapture offers a 32% advantage versus conventional chemical ($I_{sp} = 325$ s) orbit insertion, while aerobraking offers a 54% advantage. However, although aerobraking is a clear winner on this basis, the need to make a large number of passes through the Van Allen radiation belts is likely to place unacceptable demands for radiation tolerance of the spacecraft and its cargo for most applications. For this reason, therefore, aerobraking at Earth will mostly not be attempted, leaving aerocapture as the preferred alternative to propulsive orbit transfer.

CONCLUSIONS

Aerocapture has been shown to provide substantial or enabling benefits to a large number of potential missions across the Solar System compared to alternative orbit insertion techniques based on chemical propulsion, solar electric propulsion, and aerobraking. Delivery cost per unit delivered mass (\$/kg) has been the primary metric used to quantify aerocapture benefits, where the delivery cost includes all elements of the architecture from launch to orbit insertion. Of the ten planetary missions in the defined set, three were found to be enabled by aerocapture (J1, S1, and N1), five were found to be improved (V1, V2, M1, T1, and U1) and two were not found to be improved (M2, J2). The normalized delivery costs based on a heavy launch vehicle for the aerocapture-enabled or aerocapture-improved missions range from \$0.05M/kg for Mars orbiters (M1) to \$0.85M/kg for Saturn orbiters (S1). On a percentage basis, the \$/kg benefit of aerocapture ranges from a 12% reduction for the M1 mission to 100% reductions for the three enabled missions. The analysis shows that these results are not very sensitive to 30% increases in both the estimated aerocapture system mass and system cost. This suggests that even modestly performing aerocapture systems will yield

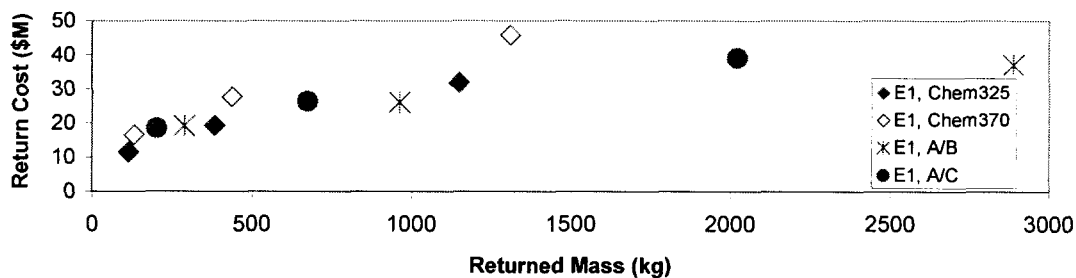


Figure 5. Results from Earth Mission E1

substantial mission benefits. An Earth mission consisting of an aeroassisted orbit transfer vehicle going from GTO to LEO showed that aerocapture offered a 32% \$/kg reduction compared to chemical propulsion. Aerobraking for this mission offered even better performance, but the problem of repeated passes through the Van Allen radiation belts are likely to preclude Earth aerobraking for most applications.

ACKNOWLEDGEMENTS

The authors would like to acknowledge the trajectory analysis assistance of Carl Sauer, Jennie Johannesen, and Theresa Debban, all at JPL. The research described in this paper was performed at the Jet Propulsion Laboratory, California Institute of Technology, under a contract with the National Aeronautics and Space Administration and administered through the In Space Propulsion Program.

REFERENCES

- ¹ M. I. Cruz, "The Aerocapture Vehicle Mission Design Concept," AIAA Paper 79-0893 presented at the Conference on Advanced Technology for Future Space Systems, Hampton, VA, May 8-10, 1979.
- ² Gerald D. Walberg, "A Survey of Aeroassisted Orbit Transfer", Journal of Spacecraft and Rockets, Vol. 22, No. 1, 1985.
- ³ W. H. Willcockson, "Mars Aerocapture Using Continuous Roll Techniques", AAS Paper 91-422, Proceedings of the AAS/AIAA Astrodynamics Conference, Durango, CO, Aug. 19-22, 1991.
- ⁴ P.F. Wecinski, W. Henline, H. Tran, F. Milos, P. Papadopolous, Y.-K. Chen, and E. Venkatapathy, "Trajectory, Aerothermal Conditions and Thermal Protection System Mass for The Mars 2001 Aerocapture Mission", AIAA Paper 97-0472, presented at the 35th Aerospace Sciences Meeting, Reno, NV, January 6-10, 1997.
- ⁵ Jeffery L. Hall, "An Overview of the Aerocapture Flight Test Experiment (AFTE)", AIAA Paper 2002-4621, presented at the AIAA Atmospheric Flight Mechanics Conference and Exhibit, Monterey, CA., Aug. 5-8, 2002.
- ⁶ Stephane Rousseau, Etienne Perot, Claude Graves, James P. Masciarelli, and Eric Queen, "Aerocapture Guidance Algorithm Comparison Campaign", AIAA Paper 2002-4822, presented at the AIAA/AAS Astrodynamics Specialist Conference and Exhibit, Monterey CA, August 5-8, 2002.

⁷ M. K. Lockwood, "Titan Aerocapture Systems Analysis", AIAA Paper 2003-4799, presented at the 39th AIAA/ASME/SAE/ASEE Joint Propulsion Conference, Huntsville, AB, July 20-23, 2003.

⁸ Bonnie James and Michelle Munk, "Aerocapture Technology Development Within the NASA In-Space Propulsion Program", AIAA Paper 2003-4654, presented at the 39th AIAA/ASME/SAE/ASEE Joint Propulsion Conference, Huntsville, AB, July 20-23, 2003.

⁹ National Academy of Science, Solar System Exploration "Decadal" Survey, July 2002.
http://www7.nationalacademies.org/ssb/SSE_Survey_Report_Part_1.pdf and
http://www7.nationalacademies.org/ssb/SSE_Survey_Report_Part_2.pdf

¹⁰
http://elvperf.ksc.nasa.gov/elvMap/staticPages/launch_vehicle_info1.html

¹¹ M. D. Rayman, "Results from the Deep Space 1 Technology Validation Mission," IAA-99-IAA.11.2.01, presented at the 50th International Astronautical Congress, October 4-8, 1999, Amsterdam, The Netherlands.

¹² J. E. Polk, et al., "In-Flight Performance of the NSTAR Ion Thruster Technology on the Deep Space One Mission," AIAA-99-2274, presented at the 35th AIAA/ASME/SAE/ASII Joint Propulsion Conference, June 21-23, 1999.

¹³ J. A. Christensen, et al., "The NSTAR Ion Propulsion System for DS1," AIAA-99-2972, presented at the 35th AIAA/ASME/SAE/ASEE Joint Propulsion Conference, Los Angeles, CA, June 1999.

¹⁴ M. J. Patterson, et al., "Next-Generation 5/10 kW Ion Propulsion Development Status," IEPC-01-089, 27th International Electric Propulsion Conference, Pasadena, CA, October 15-19, 2001.

¹⁵ M. J. Patterson, et al., "NEXT: NASA's Evolutionary Xenon Thruster," AIAA-2002-3832, presented at the 38th AIAA/ASME/SAE/ASII Joint Propulsion Conference, July 7-10, 2002, Indianapolis, IN.

¹⁶ S. Oleson, et al., "Mission Advantages of NEXT: NASA's Evolutionary Xenon Thruster," AIAA-2002-3969, presented at the 38th AIAA/ASME/SAE/ASII Joint Propulsion Conference, July 7-10, 2002, Indianapolis, IN.

¹⁷ The assumed value of 370s is somewhat higher than currently identified systems but is intended to represent a "best-case" long-term performance goal.

¹⁸ Projected specific impulse of the NeXT ion engine under development by Glenn Research Center.

¹⁹ NASA, "New Frontiers AO, ELV Launch Services Information Summary 02/25/03", page 4, 2003, <http://centauri.larc.nasa.gov/newfrontiers/AO-New Frontiers-ELV Info S 1.pdf>

²⁰ JPL, February 2003. Unpublished estimate that a Cassini bipropellant system rebuild (500 kg dry mass) would cost \$40M. The cost model gives $2 + 1.7 \times 500^{0.5} = \$40M$.

²¹ John R. Brophy, private communication, February 2003. He estimated that a 25 kw, 800 kg dry mass SEP system based on advanced NSTAR technology from DS-1 would cost \$63M. The cost model gives $40 + 0.8 \times 800^{0.5} = \$63M$.

²² Robert A. Mase, private communication. Mars Odyssey data indicates that aerobraking for the 600 kg spacecraft had a cost of \$9.3M including planning, development, operations and science team during the 3 month aerobraking period. The cost model gives $5 + 0.2 \times 600^{0.5} = \$9.9M$.

²³ Jeffery L. Hall, unpublished data from the design described in Ref. 5. The estimated cost of the AFTE aerocapture system was \$12.8M including the design, analysis, simulation, aeroshell fabrication, system integration, and testing. Since the AFTE aeroshell was approximately 50 kg, the model gives $7 + 0.8 \times 50^{0.5} = \$12.7M$.